Electronic structure of an ideal diamond-nickel (001) interface

Warren E. Pickett and Steven C. Erwin
Complex Systems Theory Branch (Code 4692), Condensed Matter and Radiation Sciences Division, Naval Research Laboratory, Washington, D.C. 20375-5000
(Received 1 December 1989)

The rapid improvement in diamond-film growth raises the possibility of constructing diamond-metal interfaces for electronic-device applications. We present calculations of the electronic structure of an idealized, lattice-matched (001) superlattice of diamond and nickel slabs, using both the linear augmented-plane-wave and linear combination of atomic orbitals methods. Eight (001) layers of C were found to be sufficient to allow the diamond valence-band edge to be well defined. For the interface atomic geometry which we have chosen, there is a large density of states at the interface within the bulk diamond band gap whose character is a nonbonding combination of adjacent C p_x, p_y and Ni d_{xz}, d_{yz} orbitals, where the interface lies in the x-y plane. The predicted Schottky-barrier height is vanishingly small. The interface electronic structure is analyzed and discussed in detail. Both the high density of interface states and the vanishing barrier height suggest that this geometry may not be optimal. A small or vanishing barrier height would, however, promote Ohmic contacts to p-type diamond.

I. INTRODUCTION

The electronic structure and atomic geometry of interfaces between covalent semiconductors and metals have been studied for silicon and germanium, as well as for some of the III-V compound semiconductors. The emphasis has been on semiconductors that are used in electronic-device (especially Schottky-device) applications, which until now has not included diamond. However, with the increasing success in growing diamond films, the character of diamond-metal interfaces becomes of great interest. More generally, diamond represents the limiting case of large-band-gap covalent semiconductors, and its behavior at the Schottky interface may help to clarify various aspects of the Schottky-barrier problem that are far from being understood.

The electronic, mechanical, and thermal properties of diamond[1] make it an ideal candidate for electronic-device applications. Its high thermal conductivity, low thermal expansion, extreme strength, and wide band gap make it a promising candidate for application as high-temperature, high-power, and/or high-frequency electronic components. Its high electron and hole mobility also are highly favorable physical attributes. Such device applications require an intimate interface between diamond and another material, either semiconductor or metal. The diamond–boron-nitride interface has been studied earlier by one of the authors.[2] In this paper we report studies of a similar nature on a diamond-metal system, specifically the (001) diamond-nickel interface.

In addition to providing insight into diamond-metal interfaces, this study bears on the important question of Schottky-barrier heights. One point of view[3,4] in the past has been that Schottky-barrier heights and their variations are determined primarily by the semiconductor, with dependence on the particular metal being secondary (described adequately by its work function). Theoretical studies of "doped" interfaces[5] showed that this was not a viable model for strongly covalent (i.e., narrow-band-gap) semiconductors, but rather that the barrier height is affected strongly by the change in electronic charge and potential at the interface. However, there is evidence that the model remains valid for ionic (i.e., wide-band-gap) materials.[6] Diamond-metal interfaces may shed new light on this controversy, since diamond is not only the prototype covalent material, but is also a wide-band-gap material, unlike the other group-IV (purely covalent) elemental semiconductors Si and Ge. We find an unusual, vanishing Schottky-barrier height (for holes) for the specific interface that we have chosen, and discuss its origin and possible implications. Experimentally, little has been reported concerning barrier heights on diamond; Sze,[7] for example, reports only a single case (for gold). Reported results for Al and Ba will be quoted later in this paper.

The paper is organized as follows. In Sec. II we provide a synopsis of experimental work on Ni-diamond systems and introduce some relevant theoretical work. The description of the interface that we have chosen to study, and its justification, are given in Sec. III. Methods of calculations are reviewed briefly in Sec. IV. In Sec. V we provide the results and a discussion of what has been learned. A brief summary of the primary results is provided in Sec. VI.

II. PREVIOUS INVESTIGATIONS

There have been several experimental studies into the C-Ni system. Growth of nickel films on diamond surfaces by vacuum deposition has been reported by Lurie and Wilson[8] and by Pavlidis.[9] Lurie and Wilson report that epitaxial nickel grows on all three low-Miller-index surfaces when the diamond substrate is held at 500–800 °C. ("Epitaxial" here indicates only that the

nickel overlayers are in registry with the substrate, since layer-by-layer deposition was not monitored.) Annealing at up to 1000 °C could improve the Ni film, but annealing at higher temperature led to graphitization and further evaporation of Ni led to island formation. Pavlidis reported vacuum deposition from 22 to 600 °C onto (001) diamond surfaces, finding mostly island or channel patterns.

Although these results seem encouraging for the formation of good diamond-Ni interfaces, there are reasons to anticipate difficulties. Recently, Davis[10] has suggested that, with few exceptions, materials with low surface energies tend to grow readily on high-surface-energy material, but not vice versa. According to Miedema,[11] Ni has a high surface energy, 0.16 eV/Å^2. This value is much higher than simple metals and is about $\frac{2}{3}$ of the upper limit for transition metals (Re,Os). Thus according to this "rule," Ni may not be as easy to grow on diamond as would lower-surface-energy metals. Diamond, however, also has a high surface energy, which will tend to promote growth of overlayers, but impede the growth of diamond as an overlayer itself.

Carbide formation at the C/Ni interface is not a likely occurrence. According to the binary Ni-C phase diagram,[12] there are no stable nickel carbides, and the mutual solubility is low even at high temperature. Thus the island formation noted above can be understood both from the lack of solubility (or carbide formation) and from the tendency of high-surface-energy materials to minimize their surface area. The ability to react with carbon and form carbides seems to be related to the tendency of diamond films to grow, since Spitsyn, Bouilov, and Derjaguin[13] have reported that the observed diamond nucleation rate on carbide-forming substrates is 1–2 orders of magnitude larger than on non-carbide-formers.

There have been a number of studies of C overlayers on Ni surfaces. Nickel is known to catalyze the formation of graphite from methane, similar to Pt and Pd. Schouten, Gijzeman, and Bootsma[14] reported that methane reacts with Ni(001) but not with Ni(111). High-vacuum deposition of C overlayers on Ni surfaces have been studied by surface extended x-ray-absorption fine structure and by angle-resolved photoemission measurements. These studies (see Sec. III) are useful from our viewpoint only for the purpose of suggesting C-Ni separations at the interface.

Finally, there is the work which in part stimulated our calculations; namely that of attempting to grow films of diamond on Ni substrates. Kasi, Kang, and Rabelais[15] reported ion-beam deposition of carbon films onto Ni(111) substrates using low-intensity, low-energy (1–300 eV) C^+ beams. The structure of the films was not firmly established, but the Auger line shape looked much more like that of cubic diamond than of graphite. The films were not thick enough to be characterized by Raman spectroscopy. Rudder *et al.*[16] have reported attempts to grow diamond films on Ni substrates using remote plasma-enhanced chemical vapor deposition (CVD). Although this technique has been successful in growing polycrystalline films on a variety of materials, their results for Ni substrates so far are negative. Belton and Schmieg[17] have also reported CVD growth of diamond films on Ni(001), but the growth was not epitaxial. Layers of graphitic carbon and disordered carbon were deposited initially, with diamond polycrystalline films forming on top of these carbon layers.

III. SELECTION OF INTERFACE

Although Cu ($a=3.61$ Å) has nearly as good a lattice match with diamond ($a=3.567$ Å) as Ni ($a=3.52$ Å), and therefore presents a good possibility for an epitaxial interface, we were led by the experimental attempts to take Ni for the initial study of a diamond-metal interface. By taking the lattice constant for nickel (6.644 a.u. $=3.515$ Å was used in our calculations) for both diamond and nickel, we simulate a situation in which diamond is grown on nickel. Although diamond overlayers which are contracted parallel to the interface to fit the nickel lattice spacing will expand somewhat in the perpendicular direction, we have not attempted to include such details in this first study. We use the same $a/4$ interlayer spacing for the diamond lattice, thus retaining perfect tetrahedral coordination of interior C atoms and thereby facilitating comparison of the charge density and density of states with that of bulk diamond.

We have taken the (001) interface for this initial study. Not only is this an easily prepared nickel face which has been used extensively in the past, it results in interface unit cells which are efficient for us to handle numerically (especially, one atom per layer). By choosing an even number of C(001) layers, a center of inversion can be retained on a bond center between the two central layers in the tetragonal cell we choose, allowing real Hamiltonian matrices.

Since the interface geometry is not known, it is necessary to come up with a reasonable model. In building a model of an epitaxial interface, it remains only to fix the relative positions of the carbon and nickel atoms on either side of the interface, and to decide on the C-Ni interlayer separation across the interface. We have fixed the relative Ni and C positions across the interface in such a way that the Ni atoms are (before increasing the C-Ni distance) in line with the diamond sp^3 dangling bonds, i.e., at C positions if the diamond structure were continued. In the language of surface science, the interface C atoms lie on a bridge site with respect to the Ni layer at the interface. The resulting supercell geometry is pictured in Fig. 1. This choice is, of course, not the only reasonable way to align the C and Ni interface layers.

Without relaxation of the C-layer–Ni-layer separation, this would make the Ni-C separation across the interface equal to the C-C separation of $(3^{1/2}/4)a=1.52$ Å, which is much too small for a C-Ni separation. Noting that the C(001)-layer separation is $a/4$, while that of Ni is $a/2$, we have taken the C-Ni interlayer separation of $0.4a$, roughly midway between these values. The resulting C-Ni separation is $(0.285)^{1/2}a=1.90$ Å.

There is some indication from studies of C adsorption on Ni that this C-Ni separation is a reasonable one. Chiarello *et al.*[18] have reported an analysis of surface-extended energy-loss fine-structure data which indicate a

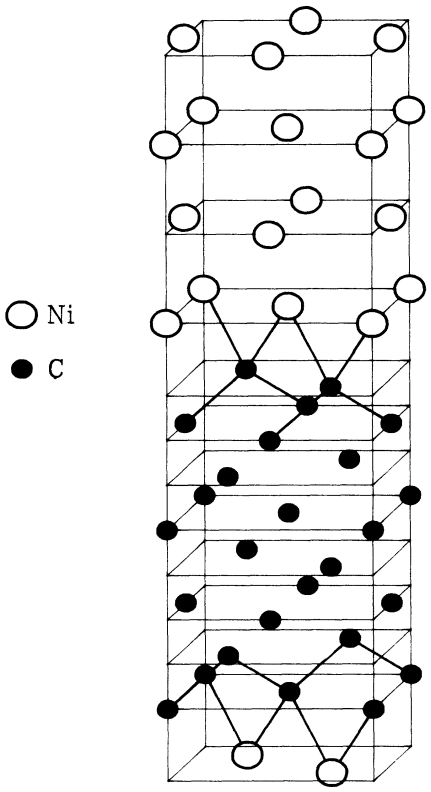

FIG. 1. The atomic geometry of the large (001) diamond-nickel superlattice used in the calculations, comprised of eight C layers and five Ni layers. For clarity, only the nearest-neighbor coordination near the interface is shown.

C-Ni separation of 1.75 Å for the C monolayer on Ni(001), and a calculation which gives 1.79 Å. Bader *et al.*[19] report values of 1.82–1.87 Å from surface-extended x-ray-absorption fine-structure data on the $p4g(2\times2)$-C/Ni(001) system. McConville *et al.*[20] have used the value 1.80 Å for a self-consistent calculation of the electronic structure of such a surface, and Jacobsen and Nørskov[21] have applied the effective-medium approach to adsorbed C on Ni and obtained values in the 1.6–1.8-Å range. Since in our case the C atom at the interface is bonded to two other C atoms, it will be less free to bond to several Ni atoms, resulting in a somewhat larger C-Ni distance than for the 50% coverage monolayer. Hence our choice of 1.90 Å seems to be a very reasonable guess.

We have studied two sizes of superlattice supercell, the first comprised of four diamond layers and three Ni layers and the second made up of eight diamond layers and five Ni layers. The coordinates of the large supercell are given in Table I, and the resulting Bravais lattice is body-centered tetragonal. The larger cell was treated because it was found that a diamond band gap was only very poorly formed by considering four layers of diamond, and the conduction- and valence-band edges could not be located at all. Finally, we have also made the simplification of neglecting the spin polarization of Ni. The primary effect of spin polarization is to redistribute charge between up spin and down spin, but not to cause charge transfer, i.e., chemical changes. The splitting of the bands can result in alterations of the bonding; however, since nickel's spin splitting is fairly small, it should not have a great effect on the chemical behavior at the interface. We expect that the interface geometry should be optimized before worrying about the effects of spin polarization.

TABLE I. Positions $(x,y,z)a$ of all inequivalent atoms in the large supercell, in units of the nickel lattice constant a. Other sites are determined by inversion symmetry through the origin and by body-centered-tetragonal translation vectors. The integer index indicates the layer with respect to the interface.

	x	y	z
C(4)	0.125	−0.625	0.125
C(3)	0.375	−0.375	0.375
C(2)	0.125	−0.125	0.625
C(1)	0.375	0.125	0.875
Ni(1)	0.125	0.375	1.275
Ni(2)	0.125	−0.125	1.775
Ni(3)	0.125	0.375	2.275

IV. METHODS OF CALCULATION

We have used two methods of calculation, the linear augmented-plane-wave (LAPW) method, which was used on both the small and large supercell, and the linear combination of atomic orbitals (LCAO) method, which has been applied only to the smaller supercell. Both methods have been applied in order to compare results, in anticipation of applications of the LCAO method, with its smaller basis set, to more extensive studies of this type. As shown below and elsewhere, the results of the two methods are in excellent agreement.

Details of the LAPW method and alogrithms as applied in our codes have been described by Wimmer *et al.*[22] and by Wei and Krakauer.[23] Sphere radii of C and Ni were 1.419 and 2.000 a.u., respectively. Angular-momentum expansions of the charge density and potential were taken up to $L=6$, and the local-density exchange-correlation potential of Hedin and Lundqvist[24] was used. (More recent, and more sophisticated, exchange-correlation parametrizations are quite similar[25] to that of Hedin and Lundqvist.) The C 1*s* and Ni 1*s*, 2*s*, 2*p*, 3*s*, and 3*p* states were treated fully relativistically as core states in the standard way. All other states were treated scalar relativistically as band states in a wide valence-band window.

The $RK_{\max}$ values were 6.0 and 8.4 referenced to the C and Ni spheres, respectively, resulting in a basis-set size (and Hamiltonian matrix size) of order 1125–1150 for the large supercell. The density was iterated to self-consistency on eight special **k** points in an irreducible $(\frac{1}{8})$ portion of the Brillouin zone. For the computation of the density of states (DOS) by the Jepsen-Andersen-Lehmann-Taut linear tetrahedron method, for the large supercell, 75 points were calculated within the irreducible zone, and these were interpolated by Fourier techniques[26]

to denser sets of points.

The general features of the LCAO method are widely known. We have used a newly developed code that is described and tested in detail elsewhere,[27] so we give here only a brief summary of the method. The LCAO basis functions are constructed from localized functions $\phi(\mathbf{r})$ in such a way as to explicitly satisfy Bloch's theorem:

$$b_{\gamma j}(\mathbf{k},\mathbf{r})=N^{-1/2}\sum_{\nu}\exp[i\mathbf{k}\cdot(\mathbf{R}_\nu+\mathbf{T}_\gamma)]\phi_{\gamma j}(\mathbf{r}-\mathbf{R}_\nu-\mathbf{T}_\gamma)\ . \tag{1}$$

Here, γ denotes the atom at position $\mathbf{T}_\gamma$ within the unit cell, and $\mathbf{R}_\nu$ is a Bravais-lattice vector. To facilitate matrix-element evaluation, each function $\phi(\mathbf{r})$ is expanded in a set of Gaussian functions, i.e.,

$$\phi(\mathbf{r})=\sum_m c_m \exp(-g_m r^2)\ . \tag{2}$$

The number of terms in this expansion is either one (for a single Gaussian function), or in the range 10–20 (for a function representing an atomic orbital). For basis functions of p or d symmetry, a corresponding angular factor multiplies the above expression. With the above definitions, all the required overlap matrix elements are expressed as sums of integrals between two simple Gaussian functions centered, in general, at different positions. These integrals can all be evaluated analytically.[28] The same procedure is easily applied to matrix elements of the kinetic-energy operator.

In order to calculate matrix elements of the potential energy, one need only express the effective (Coulomb plus exchange-correlation) potential, $V_{\rm eff}(\mathbf{r})$, as another Gaussian expansion. The resulting matrix elements can then be calculated analytically or in terms of the error function.[28] A Gaussian expansion of the potential is generated by first tabulating $V_{\rm eff}(\mathbf{r})$ on a dense mesh, subtracting off the nuclear potential spikes with functions $(Z/r)\exp(-\alpha r^2)$, then least-squares fitting the remaining (largely electronic) contribution to simple Gaussian functions. In this way, we have always been able to fit $V_{\rm eff}(\mathbf{r})$ with an error of less than 0.1 eV (rms) over the entire cell.

The effective potential itself is calculated numerically from the charge density as follows. The total electronic density is decomposed into two contributions. The first is a localized part centered on each atom, expressed as a sum of numerical radial functions multiplied by lattice harmonics, for which the associated Coulomb potential is easily calculated by one-dimensional integration. For this we have used a standard cubic spline algorithm. The second contribution is small throughout the unit cell and devoid of sharp features, and hence has a rapidly convergent Fourier series; we have used a fast-Fourier-transform procedure to calculate the contribution of this piece to the potential. A local-density approximation to the exchange-correlation potential is then calculated in the usual manner, using the total electronic density.

Finally, the charge density is constructed directly from the eigenvectors corresponding to the Hamiltonian of the previous interaction, thus providing the self-consistency link between input and output charge densities. A modified Broyden's algorithm[29] is used to accelerate the approach to self-consistency.

In our implementation of the LCAO method, basis functions are constructed from all of the occupied atomic states of the constituent atoms, plus a number of single Gaussian functions. For carbon atoms, the basis set consisted of six s-type functions, five p-type functions, and no d-type functions, which we denote by C(6/5/0). For nickel, the basis set was chosen to be Ni(7/5/3). Thus the total basis-set size, for the smaller supercell of four C and three Ni atoms, was of order 200. The Gaussian exponents used in the expansions for these basis functions were essentially chosen from Huzinaga[30] and Wachters.[31] For C, 13 exponents were used, ranging from 0.248 050 to 9470.52 a.u.; for Ni, 15 exponents ranging from 0.251 239 to 284 878 a.u. were used. For both atoms, the orbital expansion coefficients were determined in a separate calculation by minimizing the atomic total energies.

V. CALCULATIONAL RESULTS AND DISCUSSION

A. Local density of states

The calculated local DOS's (LDOS's), using the atom-centered LAPW spheres, are shown in Fig. 2 for each of

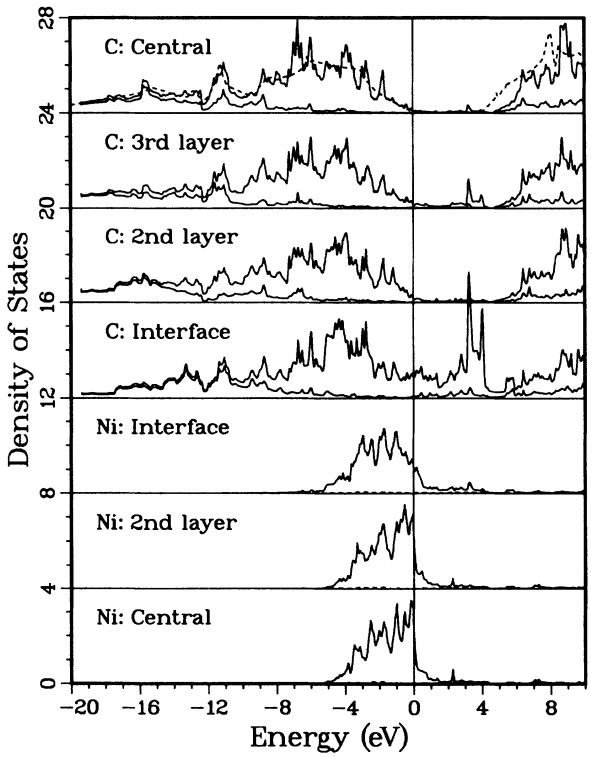

FIG. 2. Local density of states for the 5 Ni–8 C layer cell, within each of the inequivalent atomic LAPW spheres in the unit cell. The Fermi level is placed at zero energy, and for uniformity the Ni LDOS's have been *divided* by a *factor of 10* with respect to the diamond LDOS. In the carbon layers the lower solid curve is the $2s$ component and the upper curve is the total (essentially $2s+2p$). The dashed curve in the "C: Central" panel is the bulk diamond density of states, with the valence-band edge placed at zero energy as discussed in the text.

the four distinct C sites and three Ni sites in the large supercell. The central Ni layer is representative of bulk Ni, with a d-band width of somewhat more than 4 eV and displaying the distinctive sharp peak at the Fermi energy E_F very near the top of the d states. The broadening of the LDOS due to the interface is already evident on the second Ni layer, but it is not severe. The broadening is more severe at the Ni interface layer, being as broad and of a similar shape to the LDOS of a *surface* Ni atom reported by McConville *et al.*[20] Thus the presence of the two C atoms across the interface does not alter the Ni LDOS noticeably from that of the free surface, suggesting a lack of strong bonding to C atoms across the interface.

On the diamond side of the interface, the effects are felt much deeper in, with the central (fourth) C layer still not being entirely representative of bulk diamond. However, one should keep in mind that the C layers are separated by only half the Ni-layer separation, so the central (fourth) C layer is the same *distance* from the interface as the central Ni layer. The bulk DOS of diamond is shown for reference in the "C: Central" panel of Fig. 2, so it can be seen that the LDOS of the central C layer shows much more structure (which is particular to our eight-layer–five-layer cell) than in the bulk. This structure appears to be due to size quantization of the diamond-slab wave functions in the z direction.

In spite of the lack of convergence of the central LDOS to the bulk value, the band gap and valence-band maximum are rather well defined, with the conduction-band minimum somewhat less well defined. The lower edge of the gap appears to coincide with the Ni Fermi level, a point we return to in Sec. V D. The lower conduction bands, in the 5–8 eV range, appear to be pushed to somewhat higher energy with respect to the bulk by interaction with the interface.

In the third C layer from the interface there is a noticeable LDOS within the gap region 0–5 eV, which, in fact, is larger than for the second C layer. The drastic differences from bulk behavior are however confined to the C layer at the interface. The gap region is entirely filled in, with states of p character which seem to be derived from the lower conduction bands as well as from the upper valence-band region. Although it might be expected that the Ni atoms would to some extent bond with the directional sp^3 bond of the interface C (the main impetus for our choice of geometry), it turns out that the Ni atoms, in fact, provide little opportunity for bonding. The tetrahedral sp^3 bonding in diamond takes place throughout the valence band (which is more than 20 eV wide), whereas there are only Ni states to bond with in the -4 to 0 eV range. This mismatch results in "dangling-bond" states that fill the gap region on the C layer at the interface and peak strongly in the 3–4 eV region.

In addition, the character of the deep valence-band states is altered at the interface, with the p character of states below -10 eV being very small. In the bulk (and

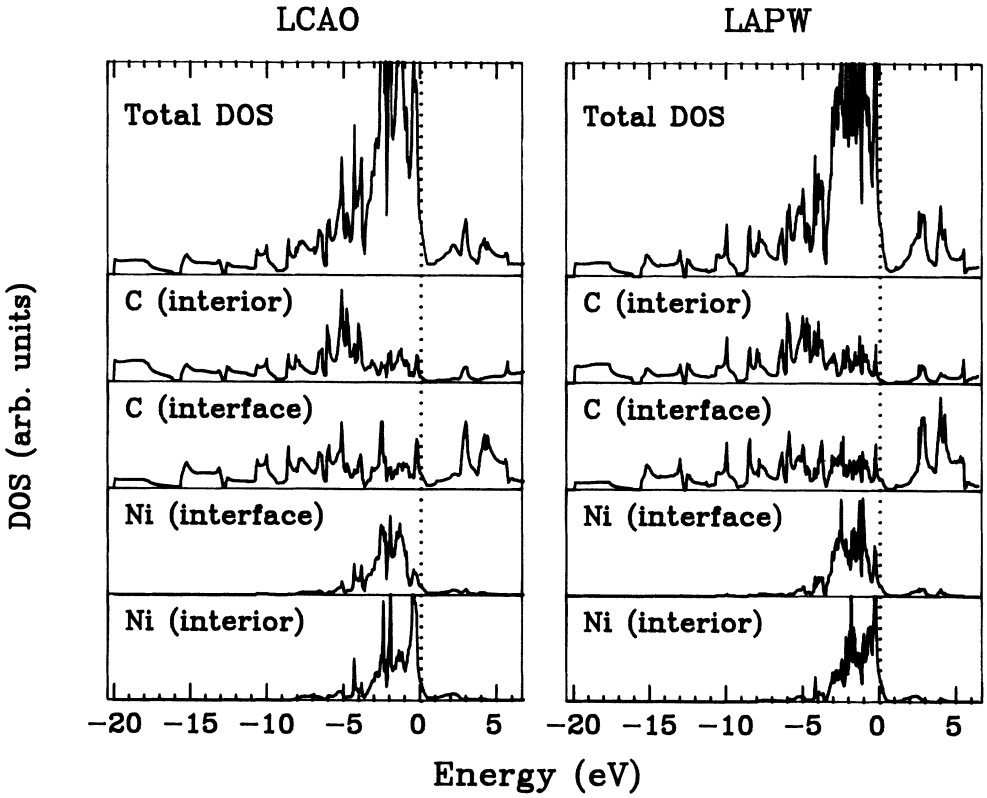

FIG. 3. Local density of states for the 3 Ni–4 C layer cell, for each of the inequivalent atoms, from both the LCAO (left-hand panel) and LAPW (right-hand panel) methods. Note that the two distinct decompositions give the same picture. The Ni LDOS is divided by approximately a factor of 10 with respect to the C LDOS.

in the central layer of this supercell) as much as 25–30 % of the character is C p down to -16 eV; the presence of the interface results in a much stronger upward shift of p character than of s character. In the conduction bands the s-to-p ratio is not changed appreciably at the interface.

For comparison, in Fig. 3 we show the LDOS's for the smaller supercell, calculated from both the LCAO and LAPW methods. Not only is the total DOS very similar, as it should be, but the LDOS's, although inequivalently defined, are also very similar. For the LCAO methods, the partial DOS's (PDOS's) shown in Fig. 3 are the Mulliken[32] populations of the local orbitals, while for the LAPW method the LDOS represents the decomposition of charge within the nonoverlapping spheres into its angular-momentum components. Evidently, for this system the projections are very similar.

The most notable feature of Fig. 3 is that the interior C atom in the four-layer slab of diamond has a "gap" in its LDOS only in the range 0–2 eV. Since the DOS both below and above this gap is not very representative of bulk diamond, the bulk band edges of diamond are not well defined by this four-C-layer slab. The discretized structure of the DOS below -10 eV, with narrow slab bands separated by gaps, also reflects size quantization of these states within the four-C-layer slab.

The interior Ni atom within the three-layer Ni slab, however, looks reasonably bulklike, with about a 4-eV bandwidth and a sharp peak just below E_F similar to that of bulk Ni. There may be a slight broadening of the LDOS of the interface Ni atom (Figs. 2 and 3), but a more noticeable effect is the small shift to lower energy of the Ni states at the interface. This shift is consistent with the charge transfer across the interface, which is discussed in the next subsection.

B. Atom charges and core-level shifts

It is possible to learn a great deal about the charge rearrangement due to self-consistency by examining the charge in each sphere and the core-level shifts near the interface. These quantities are given in Table II for the large supercell. The charge in the C sphere at the interface is 0.15 electrons less than in the central spheres, while that in the interface Ni sphere is 0.14 electrons more, indicating charge transfer across the interface from the C atom to the Ni atom. Since not all of the charge on an atom (which in any case cannot be defined precisely) lies within our LAPW spheres, it is reasonable to consider that about 0.2 electron is transferred across the interface.

TABLE II. Charges within the LAPW spheres, $Q_{\rm sph}$, and core eigenvalues E_c, for the inequivalent sites in the cell. For C the only core level is 1s, while for Ni we show the 3s eigenvalue. For clarity, the z position of the atoms is given. Site notation is as in Table I.

	z	$Q_{\rm sph}$	E_c
C(4)	0.125	4.38	−18.450
C(3)	0.375	4.38	−18.450
C(2)	0.625	4.37	−18.435
C(1)	0.875	4.23	−18.450
Ni(1)	1.275	26.49	−6.665
Ni(2)	1.775	26.37	−6.632
Ni(3)	2.275	26.35	−6.638

A physical requirement for a stable, self-consistent (isolated) metal-semiconductor interface is that the metal Fermi level lie within the band gap of the semiconductor, since otherwise there would be a nonzero concentration of electrons or holes in the semiconductor and it would not be charge neutral. A transfer of charge from the C side to the Ni side of the interface will increase the potential seen by electrons on the Ni side, and decrease the potential on the C side, compared to the situation before charge transfer. Even with this upward shift, the Fermi level of Ni lies at the bottom of the diamond gap. Thus the C-to-Ni charge transfer which has occurred at this interface is the minimum amount necessary to prevent the Ni Fermi level from falling within the diamond valence-band region.

In Table II we also show representative core eigenvalues, 1s for C and 3s for Ni. On the Ni side the expected behavior is evident—the self-consistent potential must be lower than on the central Ni atom since the charge is greater, and the lower 3s core eigenvalue (by 27 mRy) reflects such a difference. The behavior on the diamond side is less straightforward. Whereas the charge is smallest on the interface layer and monotonically and rapidly approaches the bulk value, it is only the 1s core level on the *second C layer* which differs from the rest. Apparently the reduced charge on the C layer at the interface is not due to a less attractive potential, which would raise the core levels, but rather to the change in bonding. The LDOS curve in Fig. 2 for the interface layer suggests that the cause is unoccupied "dangling-bond" states within the gap region that are derived from bonding states that are occupied in normal (tetrahedrally bonded) diamond. The character of these dangling-bond states, as well as of the valence charge density itself, is addressed in the next subsection.

C. Charge density and interface states

The character of the charge density of diamond, with its highly directional covalent bonds, is a widely recognized and well-understood property. The disruption in this covalent-bonding character at the interface can be discerned from charge-density-contour plots. At surfaces the disruption of bonding leaves "dangling bonds" which lead to states within the bulk gap which often are partially occupied,[33] and these states cause relaxations and reconstructions of the surface atoms[34,35] in order to lower the energy of the dangling-bond states. However, for the diamond-BN (110) (nonpolar) interface which we have studied[2] earlier, the two materials appeared to be similar enough that large reconstruction did not appear to be likely.

In Fig. 4 we show the valence density contours in a {110} plane of the large supercell which contains the C—C bonding chain in the two central layers as well as

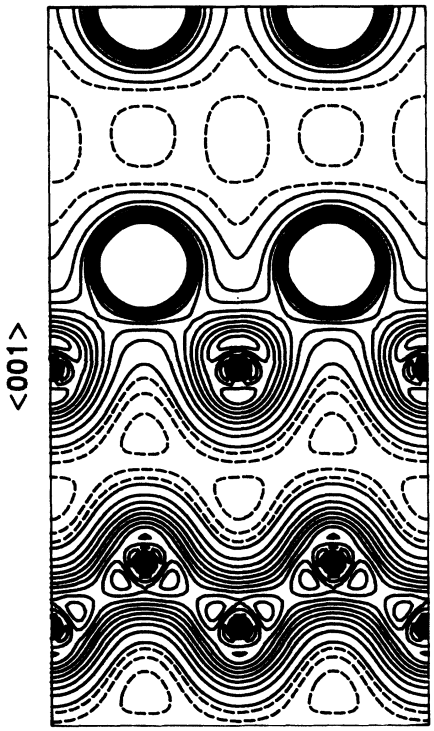

FIG. 4. Contours in a {110} plane containing the C—Ni bond of the valence charge density for the large supercell. Somewhat more than one-half of the supercell is shown; the top of the figure is at the center of the Ni slab, whereas the center of the C slab occurs midway between the two C layers forming the C—C bonding chain at the bottom. Two C layers lie out of this plane and cannot be seen. Solid circles denote the C atoms, and high-density contours around the Ni atoms have been omitted. Solid contours increase from 0.05 a.u. in units of 0.025 a.u., while dashed contours values are 0.02, 0.03, and 0.04 a.u.

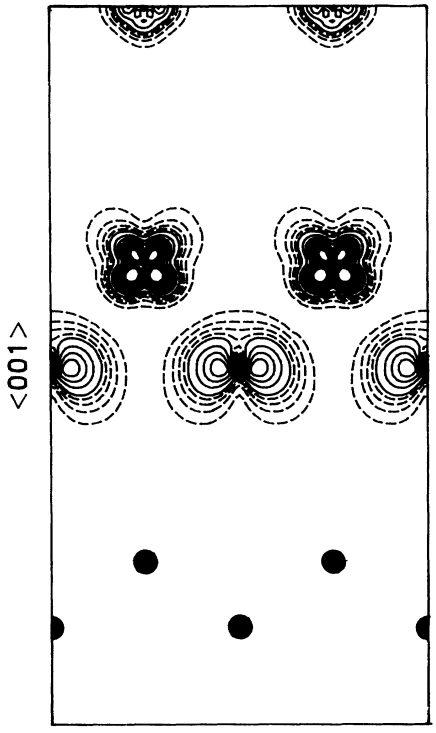

FIG. 5. Contour plot of unoccupied states with energies between 2.5 and 5.0 eV above E_F. The plane and notations are as in Fig. 4. These states involve nonbonding combinations of C p_x,p_y states and Ni d_{xy},d_{yz} states.

the corresponding C-Ni chains at the interface. The directional bonding, with peaks occurring roughly $\frac{2}{3}$ of the way to the bond center, are clearly evident in the C—C chains, and the empty channel between the chains is also obvious. In the C—Ni chain, however, there is no apparent directional C—Ni bonding; instead the high-density side of the asymmetric interface C atom which is on the Ni (interface) side indicates C p_z states which are π bonding with two Ni atoms. The interface C density in this plane is dominated by the p_z component. The interface Ni atom remains very nearly spherical, as expected from the LDOS plots of Fig. 2. Nearly all of the d states are filled in bulk Ni, leading to nearly spherical atoms. The broadening of the density of states at the interface tends to increase slightly the number of Ni d holes, but this increase is counteracted by the small downward shift of the LDOS on the Ni atom at the interface.

The preference toward C p_z-state occupation at the interface implies that more p_x,p_y states will be unoccupied. This fact is borne out by Fig. 5, where the density of unoccupied states in the large peak at 2.5–5.0 eV is plotted in the same plane of the large supercell as chosen for Fig. 4. These states are almost entirely p_x,p_y on the C, and are d_{xz},d_{yz} on the interface Ni atom. The very low density of these states midway between the C and Ni atoms indicates the states are nonbonding (or antibonding) combinations.

The distinct effect on p_x,p_y (parallel) states and p_z (perpendicular) states can be seen also from the projected LDOS on the C atoms shown in Fig. 6 for the small supercell. For the "interior" atom, which is only one layer away from the interface, there are differences in detail, but for the interface C the differences are pronounced. There is a large density of unoccupied parallel states above E_F, consistent with the charge-density plot in Fig. 5. For the occupied states, the density of states is drastically reduced in the bonding range -10 to 0 eV; many of these states are pushed up by the disruption in bonding at the interface, with the uppermost ones becoming unoccupied. The charge transfer discussed above therefore must go preferentially out of C p_x,p_y states.

D. Schottky-barrier height

For electronic-device applications the single most important property of a metal-semiconductor interface is the Schottky-barrier height, i.e., the position of the metal Fermi level with respect to the semiconductor valence-band edge. Rather little is known about barrier heights

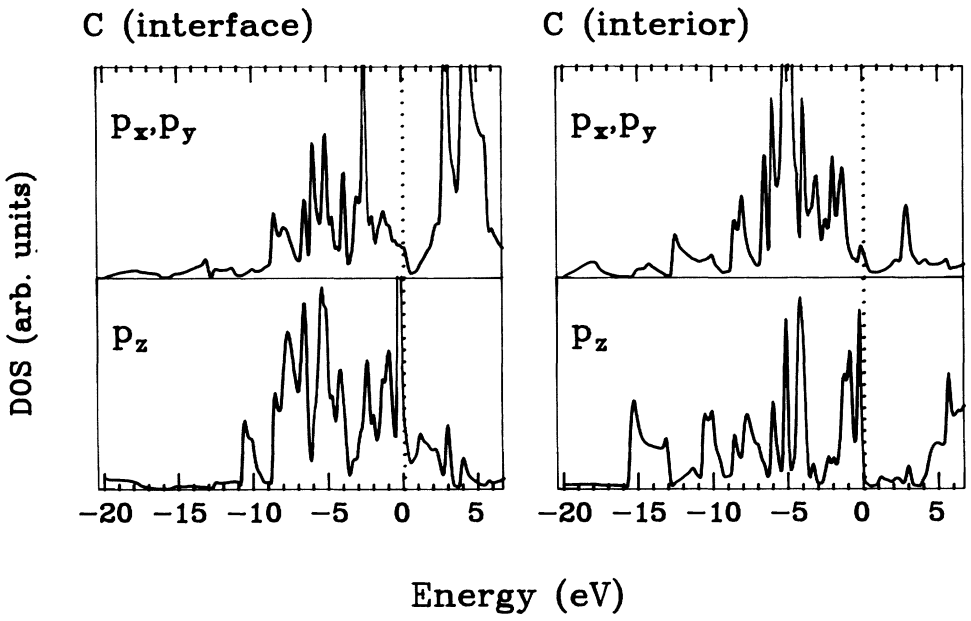

FIG. 6. Density of states for the interface and interior C atoms in the small supercell, projected onto C p_x,p_y states (upper) and the C p_z state. For the interface C atom, the p_z states are strongly preferentially occupied, in agreement with Fig. 5 that unoccupied states involve p_x,p_y states. The difference is much less pronounced for the interior atom, and the curves would be identical for a C atom in bulk diamond.

involving diamond. Values have been reported for the diamond-Au system: 1.71 eV (Ref. 7), 1.7–2.0 eV (Ref. 36), 1.3 eV (Ref. 37); for the diamond-Al system: 1.92–2.2 eV (Ref. 36), 1.5 eV (Ref. 37); and for the diamond-Ba system: 2.0 eV (Ref. 36). The variations may be due to different conditions of the interfaces as well as resulting from different measured quantities; however, all involved the (111) diamond surface rather than the (001) surface being considered here. As in most Schottky systems, the experimental barrier height is found to be a substantial fraction of the band gap of the semiconductor.

To obtain a prediction of the Schottky-barrier height for this interface, it is necessary to identify, as well as possible, the diamond band edges with respect to the Ni Fermi level. In Fig. 7 we compare the LDOS for the central C atom in the large supercell (the most bulklike layer) with that of bulk diamond. The relative normalization is somewhat arbitrary, since the LDOS is only for charge within the LAPW sphere centered on the C atom, while the bulk density of states includes the entire cell, and our normalization in Figs. 2 and 7 is made to make the areas below the valence-band curves similar. The bulk DOS in Fig. 7 is placed with the valence-band edge at zero energy, which is the Fermi level of diamond. The nonbulklike structure in the C(interior) LDOS makes it difficult to align valence-band peaks exactly, but this choice of lineup provides a reasonable representation of the edge region just below E_F (0.0 eV) as well as the general DOS structure in the -8 eV to -1 eV region. With this band lineup a vanishing Schottky-barrier height is obtained.

From both the behavior in the region -1 eV to E_F and the (apparent) conduction-band edges, it could be argued that a better lineup could be obtained by raising the bulk DOS curve for diamond by ~ 0.3–0.5 eV. However, this would result in the Ni Fermi level lying *below* the diamond valence-band edge, which cannot occur at an interface. Since a downward displacement of the bulk DOS makes the agreement worse, especially in the

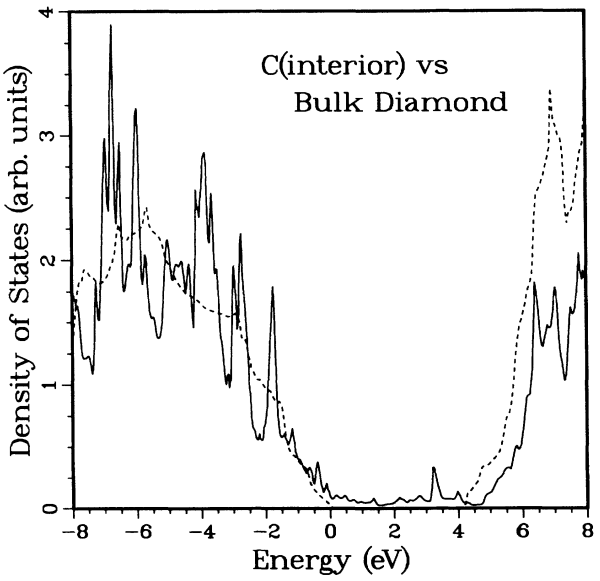

FIG. 7. Plot of the local density of states of the central C atom in the large supercell (solid), compared with the bulk diamond density of states (dashed) with the valence-band maximum placed at the supercell Fermi level. This comparison leads to a vanishingly small Schottky barrier for this interface, as discussed in the text.

conduction-band region, a zero Schottky-barrier height is the only consistent conclusion. Another factor might be the ferromagnetism of Ni, which we have disregarded in our calculations. Unlike the large exchange splitting in iron, ferromagnetism in Ni leads only to rather small exchange splittings (0.5–0.7 eV) of the Ni bands and to second-order changes in bonding, so we do not expect important magnetic contributions to the barrier height. The prediction, then, is of a barrier height very near zero for the geometry we have chosen.

One possible conclusion one might draw from the vanishing Schottky-barrier height for this interface is that the geometry is significantly different than optimal. Certainly, layer relaxation in the geometry we have chosen could lead to electron-volt size changes in the band lineups at the interface, while interface reconstruction or a relative lateral shifting of the nickel and diamond lattices could lead to qualitatively different bonding in the interfacial region and to a very different barrier height. Another possibility is that a small barrier height encourages charge fluctuations across the interface much more than would occur for a large barrier height, and therefore promotes instabilities for those atomic geometries which lead to a small or vanishing barrier height.

On the other hand, a small Schottky barrier may be a desirable property, especially for diamond. One fundamental difficulty with applications of diamond in electronic applications is that Ohmic contacts to diamond are very difficult to fabricate. A small, or ideally a vanishing, barrier height should be most conducive to promoting Ohmic contacts to p-type diamond, since the potential barrier becomes small or zero. In the light of the models of Schottky-barrier heights which invariably lead to values which are an appreciable fraction of the energy gap, it is important to determine how barrier height depends on the interfacial atomic geometry, and specifically what characteristics of this interface are responsible for the vanishing barrier height. We are continuing studies with these questions in mind.

It is common to compare the Schottky-barrier height to the differences in work functions ϕ of the two materials, although this "zeroth-order" approximation often is not accurate. The value for Ni is $\phi(\mathrm{Ni})=4$ eV, but the work function of diamond is not very well known. Ihm *et al.*[33] calculated 7 eV (with estimated 10% accuracy) for an unreconstructed (111) surface, while Pate[35] quotes a value of 0.0 ± 0.2 eV for an experimental value for the *electron affinity* of the polished (111) surface. Himpsel *et al.*[37] have suggested a negative electron affinity (conduction-band edge above the vacuum level) for certain diamond surfaces; however, this apparently is not the case for intrinsic diamond surfaces.

With a gap of 5.5 eV, the experimental value of 0.0 eV for the electron affinity suggests a value $\phi(\mathrm{diamond})=5.5$ eV. This "zeroth-order" estimate then gives a Schottky-barrier height of $(5.5-4)$ eV $=1.5$ eV, corresponding roughly to the reported barrier heights (none of which involve nickel, however). This is much larger than our calculated value, but this simple estimate is certainly not to be relied on. Until measurements are made on the diamond-Ni(001) system, however, it cannot be concluded that our calculated vanishing barrier height signifies an unrealistic atomic geometry for this system.

VI. SUMMARY

We have carried out the first self-consistent study of the electronic bonding and structure of a diamond-nickel interface, using two supercell sizes and two methods of calculation (LAPW and LCAO). Since no experimental information exists on the atomic geometry of a (001) interface between these two materials, we have made a reasonable choice based on preserving the tetrahedral coordination of carbon atoms at the interface. In principle, the geometry should be relaxed to minimize the energy, an extension we have not carried out yet. In fact, we expect to test at least one other choice of interface geometry (in which tetrahedral coordination is not so well preserved) before making the more extensive investigations of geometry optimization.

The local density of states indicates that at the third layer from the interface the Ni environment is close to that of the bulk, while on the fourth carbon layer from the interface there are still considerable deviations from the diamond bulk. Due to the narrow d-band width of Ni, the broad sp^3 bonding in diamond is disrupted at the interface, in spite of the (approximate) tetrahedral coordination of the C atom. As a result, normally bonding C p states at the interface are pushed up into the diamond gap, leading to a large density of unoccupied nonbonding C p_x,p_y – Ni d states 0–5 eV above the occupied states.

The calculated Schottky-barrier height is essentially zero. This value is substantially smaller than values reported for a few other metals on diamond, and may signal a real or incipient instability of the interface geometry we have chosen. If a very small barrier height could be achieved, however, it should promote the fabrication of Ohmic contacts to p-type diamond, which has been a crucial consideration in the possible application of diamond in electronics applications.

ACKNOWLEDGMENTS

We are grateful to H. Krakauer and D. Singh for discussions and assistance with computational procedures. Conversations with M. R. Pederson and K. A. Jackson about numerical methods have been very helpful, and we have had helpful comments from B. M. Klein and M. Yoder. One of us (S.E.) acknowledges financial support from the National Research Council. This work was supported by the Innovative Science and Technology Program of the Strategic Defense Initiative Office, administered through the Office of Naval Research. Calculations were carried out on the Cray Research, Inc. X-MP/24 supercomputer at the Naval Research Laboratory and the IBM 3090 supercomputer at the Cornell National Supercomputing Facility.

[1]*The Properties of Diamond,* edited by J. E. Field (Academic, London, 1979).
[2]W. E. Pickett, Phys. Rev. B **38**, 1316 (1988).
[3]S. Kurtin, T. C. McGill, and C. A. Mead, Phys. Rev. Lett. **22**, 1433 (1970).
[4]J. Tersoff, Phys. Rev. B **32**, 6968 (1985).
[5]S. B. Zhang, M. L. Cohen, and S. G. Louie, Phys. Rev. B **32**, 3955 (1985).
[6]For a comprehensive review, see L. J. Brillson, Surf. Sci. Rep. **2**, 123 (1982).
[7]S. M. Sze, *Physics of Semiconductor Devices* (Wiley-Interscience, New York, 1981), p. 291.
[8]P. G. Lurie and J. M. Wilson, Surf. Sci. **65**, 453 (1977).
[9]P. Pavlidis, Thin Solid Films **42**, 221 (1977).
[10]R. Davis (unpublished).
[11]A. R. Miedema, Z. Metallkd. **69**, 287 (1978).
[12]*Binary Alloy Phase Diagrams,* edited by T. B. Massalski (American Society for Metals, Metals Park, OH, 1986), Vol. 2, p. 578.
[13]B. V. Spitsyn, L. L. Bouilov, and B. V. Derjaguin, J. Cryst. Growth **52**, 219 (1981).
[14]F. C. Schouten, O. L. J. Gijzeman, and G. A. Bootsma, Surf. Sci. **87**, 1 (1979).
[15]S. Kasi, H. Kang, and J. W. Rabalais, Phys. Rev. Lett. **59**, 75 (1987).
[16]R. A. Rudder, J. B. Posthill, G. C. Hudson, M. J. Mantini, and R. J. Markunas, in *Diamond Optics,* edited by A. Feldman and S. Holly (SPIE, Bellingham, WA, 1989), Vol. 969, p. 72.
[17]D. N. Belton and S. J. Schmieg, J. Appl. Phys. (to be published).
[18]G. Chiarello, J. Andzelm, R. Fournier, N. Russo, and D. R. Salahub, Surf. Sci. **202**, L621 (1988).
[19]M. Bader, C. Ocal, B. Hillert, J. Haase, and A. M. Bradshaw, Phys. Rev. B **35**, 5900 (1987).
[20]C. F. McConville, D. P. Woodruff, S. D. Kevan, M. Weinert, and J. W. Davenport, Phys. Rev. B **34**, 2199 (1986).
[21]K. W. Jacobsen and J. K. Nørskov, Surf. Sci. **166**, 539 (1986).
[22]E. Wimmer, H. Krakauer, M. Weinert, and A. J. Freeman, Phys. Rev. B **24**, 864 (1981).
[23]S.-H. Wei and H. Krakauer, Phys. Rev. Lett. **55**, 1200 (1985).
[24]L. Hedin and B. I. Lundqvist, J. Phys. C **4**, 2064 (1971).
[25]See, for example, Appendix B of the review by W. E. Pickett, Comput Phys. Rep. **9**, 115 (1989).
[26]W. E. Pickett, H. Krakauer, and P. B. Allen, Phys. Rev. B **38**, 2721 (1988).
[27]S. C. Erwin, M. R. Pederson, and W. E. Pickett, Phys. Rev. B (to be published).
[28]W. Y. Ching, C. C. Lin, and D. L. Huber, Phys. Rev. B **14**, 620 (1976).
[29]C. G. Broyden, Math. Comput. **19**, 577 (1965); D. D. Johnson, Phys. Rev. B **38**, 12 807 (1988).
[30]S. Huzinaga, J. Chem. Phys. **42**, 1293 (1965).
[31]A. J. H. Wachters, J. Chem. Phys. **52**, 1033 (1970).
[32]R. S. Mulliken, J. Chem. Phys. **23**, 1833 (1955).
[33]J. Ihm, S. G. Louie, and M. L. Cohen, Phys. Rev. B **17**, 769 (1978).
[34]D. Vanderbilt and S. G. Louie, J. Vac. Sci. Technol. B **1**, 723 (1983).
[35]B. B. Pate, Surf. Sci. **165**, 83 (1986).
[36]C. A. Mead and T. C. McGill, Phys. Lett. **58A**, 249 (1976).
[37]F. J. Himpsel, P. Heimann, and D. E. Eastman, Solid State Commun. **36**, 631 (1980); F. J. Himpsel, D. E. Eastman, and J. F. van der Veen, J. Vac. Sci. Technol. **17**, 1085 (1980).